Wasiuk, D. K., Khan, M. A. H., Shallcross, D. E., Derwent, R. G., & Lowenberg, M. H. (2016). A mitigation strategy for commercial aviation impact on NO_x-related O_3 change. *Journal of Geophysical Research: Atmospheres*, *121*(14), 8730-8740. https://doi.org/10.1002/2016JD025051

AGU PUBLICATIONS

JGR

Journal of Geophysical Research: Atmospheres

RESEARCH ARTICLE

10.1002/2016JD025051

Key Points:

- Global aviation CO and hydrocarbons emissions are reduced by 79% and 21% with the mitigation strategy
- NO_x and O_3 are reduced near tropopause when turbofans are replaced by turboprops
- The replacement strategy results in a reduction of ground-level aviation CO and NO_x emissions by 33 and 29%, respectively

Correspondence to:
M. H. Lowenberg,
m.lowenberg@bristol.ac.uk

Citation:
Wasiuk, D. K., M. A. H. Khan, D. E. Shallcross, R. G. Derwent, and M. H. Lowenberg (2016), A mitigation strategy for commercial aviation impact on NO_x-related O_3 change, *J. Geophys. Res. Atmos.*, *121*, 8730–8740, doi:10.1002/2016JD025051.

Received 7 MAR 2016
Accepted 11 JUL 2016
Accepted article online 15 JUL 2016
Published online 29 JUL 2016

A mitigation strategy for commercial aviation impact on NO_x-related O_3 change

D. K. Wasiuk[1], M. A. H. Khan[2], D. E. Shallcross[2], R. G. Derwent[3], and M. H. Lowenberg[1]

[1]Department of Aerospace Engineering, Queen's Building, University of Bristol, Bristol, UK, [2]Atmospheric Chemistry Research Group, School of Chemistry, University of Bristol, Bristol, UK, [3]RD Scientific, Newbury, UK

Abstract An operational mitigation strategy for commercial aircraft impact on atmospheric composition, referred to as the turboprop replacement strategy (TRS), is described in this paper. The global air traffic between 2005 and 2011 was modeled with the TRS in which turbofan powered aircraft were replaced with nine chosen turboprop powered aircraft on all routes up to 1700 nautical miles (NM) in range. The results of this TRS double the global number of departures, as well as global mission distance, while global mission time grows by nearly a factor of 3. However, the global mission fuel and the emissions of aviation CO_2, H_2O, and SO_x remain approximately unchanged, and the total global aviation CO, hydrocarbons (HC), and NO_x emissions are reduced by 79%, 21%, and 11% on average between 2005 and 2011. The TRS lowers the global mean cruise altitude of flights up to 1700 NM by ~2.7 km which leads to a significant decrease in global mission fuel burn, mission time, distance flown, and the aircraft emissions of CO_2, CO, H_2O, NO_x, SO_x, and HC above 9.2 km. The replacement of turbofans with turboprops in regional fleets on a global scale leads to an overall reduction in levels of tropospheric O_3 at the current estimated mean cruise altitude near the tropopause where the radiative forcing of O_3 is strongest. Further, the replacement strategy results in a reduction of ground-level aviation CO and NO_x emissions by 33 and 29%, respectively, between 2005 and 2011.

1. Introduction

Short-haul flight (intracontinental and domestic missions) accounted for 92% of all global departures recorded, and over a half of the estimated total global emissions of CO_2 and NO_x between 2005 and 2011 [*Wasiuk*, 2014]. The short-haul flight generally climbs out to the desired cruise altitude, spends a relatively small proportion of the total mission time in cruise, and descends [*Erzberger et al.*, 1975]. However, long-haul missions (mostly intercontinental) require the aircraft to carry large volumes of fuel on board contributing to an increased aircraft weight, which in turn leads to higher fuel burn and emissions [*Wasiuk et al.*, 2015]. In terms of fuel consumption, climb is the most expensive part of any flight. Flight is always more efficient in cruise as, by design, the cruise altitude is the altitude at which aircraft burn the least amount of fuel. Propulsion for most commercial aviation aircraft is provided by turbofan or turboprop engines. Both are air-breathing engines in which the turbine produces work to run the compressors: in a turbofan, the turbine also rotates the fan-housed upstream of the hot section of the engine, and this fan produces most of the thrust; in a turboprop, the turbine drives a propeller which generates the majority of the thrust. Turboprop aircraft are better suited than turbofan for short-haul missions as they spend more time in cruise and are noted for their low fuel consumption [*Babikian et al.*, 2002]. But the efficient technology (e.g., turboprop) was abandoned in favor of the less efficient and less environmentally friendly technology (e.g., turbofan) in the 1980s because of the low fuel cost, the advantage of higher flight speeds, and hence utilization. Turbofans are also chosen in favor of turboprops due to a "level of passenger service in the form of comfort and perceived safety" [*Ryerson and Hansen*, 2010]. The findings in *Ryerson and Hansen* [2010] indicated that rising fuel prices could reverse this trend in the short-haul markets, and they concluded that high fuel costs could potentially overshadow the importance of passenger convenience. There is a dramatic drop in fuel cost over recent years; however, the environmental cost could tip the advantage in favor of the turboprop. This can be coupled with the findings on the availability of fuel by *Nygren* [2008] which suggest that aviation fuel production is predicted to decrease by several percent a year after the crude oil production peak is reached. The growth in demand for air traffic, coupled with falling availability of aviation fuel, "envisages a substantial lack of jet fuel by the year 2026."

Nowadays, the majority of missions are operated using turbojet and turbofan equipped aircraft. Thus, the technology (e.g., turboprop) available to us is not being used in the most efficient way possible, i.e., using the least amount of energy. Recent years have witnessed a shift away from turboprops toward regional turbofans, which on a per seat basis are less fuel efficient [*Ryerson and Hansen*, 2010]. This represents in a significant move away from a more environmentally beneficial option. If turboprop aircraft can be utilized on short-haul missions instead of turbofans, there is potential for increasing fuel efficiency of regional air traffic on a regional as well as global scale. Such a substitution across regional fleets on a global scale would cause the global mean cruising altitudes to be lowered.

The aircraft emissions of NO_x, CO, hydrocarbons (HC), and particles are of concern in terms of local air quality [*Yu et al*., 2004; *Peace et al*., 2006], and the emissions of CO_2, H_2O, NO_x, SO_x and particles are of concern in terms of global climate change [*Rogers et al*., 2002; *Köhler et al*., 2013; *Gilmore et al*., 2013; *Skowron et al*., 2015]. Aircraft emissions of CO_2 and H_2O released at commercial cruise altitudes can contribute directly to climate change by increasing the levels of greenhouse gases in the upper troposphere and lower stratosphere. Aircraft NO_x emissions have an indirect effect on our climate via tropospheric O_3 production and through removal of CH_4 [*Olsen et al*., 2013; *Wasiuk et al*., 2016a]. Aircraft SO_x emissions can be oxidized in the atmosphere to form sulfate aerosol particles, which also contribute to climate change (notably through cooling) [*Pitari et al*., 2002]. Contrails from aircraft engines increase cloud cover directly or indirectly causing a positive mean radiative forcing at the top of the troposphere [*Schumann*, 2002; *Burkhardt and Kärcher*, 2011].

Utilizing a turboprop instead of a turbofan on a short-haul mission reduces CO_2 and NO_x emissions because of the lower fuel burn [*Babikian et al*., 2002]; thus, there is a potential for environmental and atmospheric benefit in substituting turbofans with turboprops on short-haul missions. An 8% of all global departures between 2005 and 2011 were estimated as long-haul departures, but this 8% accounted for nearly half of the total global mission fuel burn, CO_2 and NO_x emissions in this time period [*Wasiuk*, 2014]. Moreover, between 2005 and 2011 long-haul departures increased continuously, by ~40% in total [*Wasiuk*, 2014]. In the light of these findings, a substitution of turbofans with turboprops on long-haul missions could potentially generate a significant saving in terms of the fuel burn, CO_2, and NO_x emissions. Due to the lack of a design specification for a possible future long-range turboprop aircraft, we investigated a scenario in this study where all turbofans were replaced only on short-haul routes with existing turboprop aircraft.

In our recent study [*Wasiuk et al*., 2015, 2016b], Aircraft Performance Model Implementation (APMI) software containing a database of global aircraft movements, a model of aircraft performance for all phases of flight and an aircraft emissions estimation method was used to create a 4-D Aircraft Fuel Burn and Emissions Inventory for the time period of 2005 to 2011. In this study, the replacement of nine selected turbofan aircraft by turboprops for flights up to 1700 nautical miles (NM) was made to build an amended 4-D Aircraft Fuel Burn and Emissions Inventory, referred to as the turboprop replacement strategy (TRS) inventory for short. Fuel burn and emissions of flights over 1700 NM were unchanged in the TRS inventory. The resulting emissions were redistributed and the global seasonal TRS 3-D NO_x Emissions Distribution Fields were created. These NO_x fields were used as an input into the 3-D global Lagrangian chemical transport model (CTM); STOCHEM-CRI and sensitivity simulations (SS) were performed for each year between 2005 and 2011 to investigate the impact of TRS relative to the reference inventory on tropospheric composition. In this study, the estimates of the mission fuel burn, mission time, mission distance, and the emissions of CO_2, CO, H_2O, HC, NO_x, and SO_x due to the replacement of turbofans on short-haul missions by a current make of turboprop airliner were compared with those due to the original fleet. The global burden and tropospheric distribution of NO_x and O_3 under the TRS is also compared with that due to the original fleet.

2. Methods

2.1. Four-Dimensional TRS Aircraft Fuel Burn and Emissions Inventory

The air traffic movement statistics database from 2005 to 2011 was mined from the global airline schedules data, CAPSTATS (http://www.capstats.com/). The Aircraft Performance Model Implementation (APMI) described in *Wasiuk et al.* [2015] was used to generate a 4-D TRS Aircraft Fuel Burn and Emissions Inventory from the aircraft database. In the TRS inventory, all unique route and aircraft combinations with a mission distance $\leq$ 1700 NM (3148 km) were extracted for the time period of 2005 to 2011 and classified according to the aircraft type (turbofan/turboprop) used on the routes as summarized in Figure 1. Each unique route with a mission distance $\leq$ 1700 NM serviced with a turbofan was considered for replacement. Nine turboprops from an aircraft database were selected to be used as the replacement aircraft. International Civil Aviation Organization

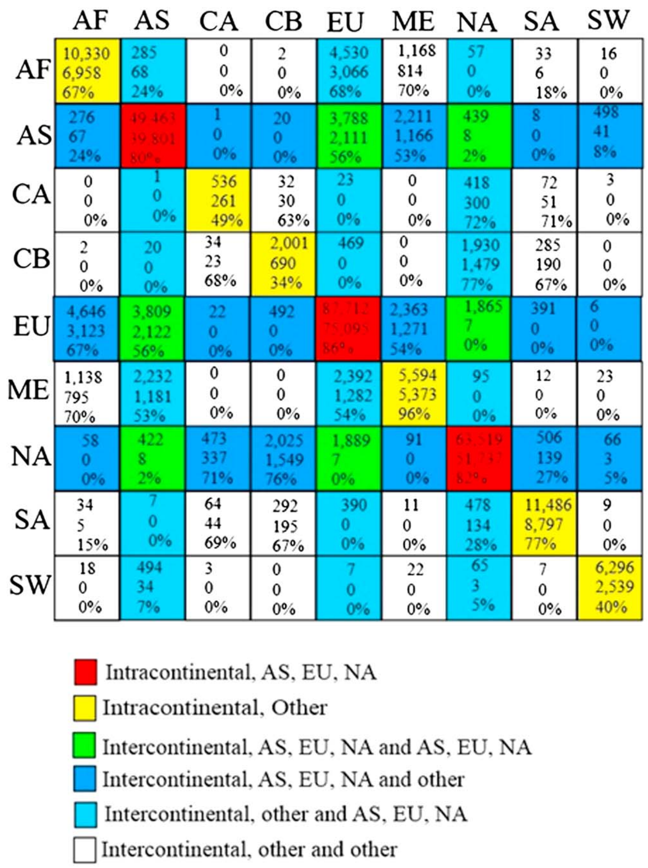

Figure 1. TRS route replacement details. The top figure in each square is the number of unique route/aircraft combinations, the middle figure is the number of unique route-turbofan aircraft combinations with a mission distance ≤ 1700 NM, and the bottom figure is the percentage of the unique route-turbofan aircraft combinations with a mission distance ≤ 1700 NM out of the total number of unique routes and aircraft combinations. The bottom figure is the proportion of the routes in each category on which an aircraft type replacement was made. (Note: AS, EU, NA, AF, CA, CB, ME, SA, SW represent Asia, Europe, North America, Africa, Central America, Caribbean, Middle East, South America, and Australia, respectively.)

(ICAO) aircraft code, aircraft name, engine name, and passenger capacity of each of the nine turboprop replacement aircraft were extracted from *SKYbrary* [2016] and cruise ranges of the replacement aircraft (in NM) were extracted from *EUROCONTROL* [2016] (Table 1). Only turboprop aircraft with a passenger capacity greater than 40 were selected in order to minimize the number of departures necessary to carry the original volume of passengers. All unique routes and turbofan aircraft combinations selected for replacement were parsed and all unique input parameter triples (the ICAO aircraft code, the mission type, and the mission distance) were extracted. Mission type and mission distance duplicates were removed, and each unique pair was assigned a turboprop from the turboprop aircraft available for replacement.

The new parameter triples in TRS were used as input into the APMI which assigned mission fuel burn and the emissions of CO_2, CO, H_2O, HC, NO_x, and SO_x to a simulated flight trajectory. The output from the APMI was used to update all the entries in the reference case (RC) inventory (the inventory with the original fleet composition) that were selected for replacement. A multiplication factor was used to calculate the number of turboprop departures required on each route selected for replacement in order to transport approximately the same volume of passengers as with the turbofans. The original number of departures associated with a unique route and aircraft combination selected for replacement was adjusted according to

Table 1. TRS Turboprop Replacement Aircraft ICAO Code, Name, Engine Name, Capacity, and Cruise Range

ICAO Aircraft Code	Aircraft Name	Engine Name	Cruise Range (NM)	Passenger Capacity
AT43	Alenia ATR-42-300/320	PW120	1700	42
AT45	Alenia ATR-42-500	PW127	1000	42
AT72	Alenia ATR-72	PW127E	1500	66
ATP	British Aerospace ATP	PW127D	1000	66
DH8C	Bombardier Dash 8 Q300	PW123	1000	52
DH8D	Bombardier Dash 8 Q300	PW150A	1300	72
F27	Fokker F-27 Friendship	PW127B	1500	46
F50	Fokker F-50	PW127B	1900	52
SB20	Saab 2000	AE2100A	1200	52

$$\text{departures}_{tp} = \frac{\text{capacity}_{tf}}{\text{capacity}_{tp}} \times \text{departure}_{tf} \tag{1}$$

where departures_{tp} is the adjusted number of departures, capacity_{tf} is the passenger capacity of the turbofan used on route, capacity_{tp} is the capacity of the turboprop selected as the replacement aircraft, and departures_{tf} is the original number of departures made on route with the turbofan.

The total global aircraft NO_x emissions in the TRS inventory were distributed on a 3-D 5° latitude × 5° longitude grid resolution [*Wasiuk et al.*, 2016b]. The vertical grid resolution followed the pressure levels and approximate height bands which are based on the vertical model resolution of the 3-D STOCHEM-CRI chemistry transport model [*Collins et al.*, 1997; *Utembe et al.*, 2010]. The nine height bands across the 5° × 5° grid result in the physical transport system in the STOCHEM model comprising 50,000 constant mass air parcels, the centroids of which were advected, on a three hour time step, through the model [*Collins et al.*, 1997; *Derwent et al.*, 2008]. The advection of the parcels was on Lagrangian trajectories, using meteorological data provided by the UK Met Office. The chemical processes that occurred within the air parcel, together with emission, deposition, mixing, and removal processes were uncoupled from transport processes to enable local determination of the chemistry time step [*Utembe et al.*, 2010]. In previous studies [*Stevenson and Derwent*, 2009; *Stevenson et al.*, 2004], STOCHEM was successfully used for measuring the impact of aviation NO_x emissions on climate. In this study, the new chemical mechanism is added in STOCHEM which is the Common Representative Intermediates mechanism version 2 and reduction 5 (CRI v2-R5), referred to as "STOCHEM-CRI." The detailed description of the CRI v2-R5 mechanism is given by *Jenkin et al.* [2008], *Watson et al.* [2008], and *Utembe et al.* [2009, 2010]. The emission totals of 27 species including CO, NO_x, and nonmethane hydrocarbons employed in STOCHEM-CRI were adapted from the Precursor of Ozone and their Effects in the Troposphere inventory [*Granier et al.*, 2005]. Emission totals for CH_4 were taken from the inverse model study of *Mikaloff-Fletcher et al.* [2004], except for the ocean emissions which were taken from *Houweling et al.* [2000]. More details about the global emission data used in STOCHEM-CRI can be found in *Khan et al.* [2014] and *Wasiuk et al.* [2016a].

The adjusted aircraft NO_x emissions from 2005 to 2011 estimated by the TRS 4-D Aircraft Fuel Burn and Emissions inventory were normalized to give global yearly aviation NO_x emissions as an input to STOCHEM-CRI. A set of seven sensitivity simulations based on the volume and distribution derived from air traffic movements recorded between 2005 and 2011 were performed in which a detailed 3-D spatial distribution of the global annual aviation NO_x emissions used as input into the CTM was modified to reflect the changes resulting from the replacement of turbofans with turboprops in regional fleets on a global scale. All simulations were run with meteorology from 1998 for a period of 24 months with the initial 12 months being discarded as a spin-up year. Three sets of results were obtained from the study: a TRS Inventory, global seasonal TRS 3-D NO_x Emissions Distribution Fields, and TRS STOCHEM-CRI sensitivity simulation (SS) results. These are presented and compared with the reference case (RC) inventory.

3. Results and Discussion

3.1. Global Changes in the Fuel Requirement and Emissions Under the TRS

The absolute and percent changes in the estimated global total number of departures, distance flown, mission time, mission fuel, and the aviation CO_2, CO, H_2O, HC, NO_x, and SO_x emissions resulting under the TRS during the time period 2005–2011 are given in Table 2. The total global number of departures required under the TRS in order to transport the same volume of passengers doubles, as does the mission distance, while the mission time grows by nearly a factor of 3. However, the mission fuel burn reduces by a small amount (0.4%) on average between 2005 and 2011 under the replacement of turbofan by turboprop on short-haul missions. An increasing fuel burn would be expected because of the annual increment in departures from 2005 to 2011, but the turbine used on a turboprop burns 25–40% less fuel compared with an equivalent turbofan engine on short-haul missions per unit thrust [*Air Transport Action Group*, 2010; *Mrazova*, 2013]. These combined effects lead to a saving in the total global mission fuel in 2005 under the TRS which turns into a gain from 2009 onward as shown in Table 2. Consequently, on average between 2005 and 2011, there is negligible change in the total global mission fuel burn under the TRS despite a doubling of the total global number of departures. It should be noted that the doubling of number of departures in this theoretical mitigation strategy arises from the consideration here of existing turboprop aircraft, which have limited payload capacities

Table 2. Absolute and Percent Changes in the Estimated Global Annual Total Number of Departures, Mission Distance, Mission Time, Mission Fuel Burn, and the Emission of CO_2, CO, H_2O, HC, NO_x, and SO_x Under the TRS During 2005 to 2011[a]

Year	Departures (10^6)	Mission Distance (10^6 km)	Mission Time (10^6 h)	Mission Fuel Burn (Tg)	CO_2 (Tg)	CO (Tg)	H_2O (Tg)	HC (Tg)	NO_x (Tg)	SO_x (Tg)
2005	31.8 (112)	36381 (116)	102.8 (183)	−2.8 (−1.9)	−8.8 (−1.9)	−0.25 (−33)	−3.5 (−1.9)	−0.24 (−85)	−0.40 (−12)	−0.002 (−1.9)
2006	32.7 (113)	37731 (115)	106.4 (183)	−2.2 (−1.5)	−7.0 (−1.5)	−0.20 (−27)	−2.8 (−1.5)	−0.20 (−82)	−0.41 (−12)	−0.002 (−1.5)
2007	35.0 (115)	40581 (116)	114.4 (185)	−1.7(−1.1)	−5.5 (−1.1)	−0.18 (−24)	−2.1 (−1.1)	−0.18 (−81)	−0.43 (−12)	−0.001 (−1.1)
2008	35.4 (116)	41130 (115)	116.0 (185)	−0.9 (−0.6)	−2.9 (−0.6)	−0.16 (−22)	−1.1 (−0.6)	−0.17 (−79)	−0.43 (−11)	−0.001 (−0.6)
2009	34.8 (117)	40669 (117)	114.4 (188)	0.3 (0.2)	1.1 (0.2)	−0.12 (−17)	0.4 (0.2)	−0.14 (−77)	−0.42 (−11)	0000 (0.2)
2010	36.2 (118)	42836 (118)	120.2 (190)	1.3 (0.8)	4.0 (0.8)	−0.10 (−15)	1.6 (0.8)	−0.13 (−76)	−0.43 (−11)	0.001 (0.8)
2011	38.2 (120)	45518 (118)	127.3 (191)	2.3 (1.3)	7.2 (1.3)	−0.08 (−12)	2.8 (1.3)	−0.12 (−73)	−0.44 (−11)	0.002 (1.3)
Mean	34.9 (116)	40629 (117)	114.5 (186)	−0.5 (−0.4)	−1.7 (−0.4)	−0.20 (-21)	−0.7 (−0.4)	−0.20 (−79)	−0.40 (−11)	0001 (−0.4)

[a]Percent changes are in parentheses.

(roughly half that of the average for the shorter-range turbofan aircraft they are replacing). A practical strategy would entail the design and operation of larger-capacity turboprop aircraft so that number of departures would not double: hence, air traffic management problems would not be incurred; fuel burn and operating costs would be lower than the theoretical approach. From the perspective of emissions, too, the doubling of departures represents a conservative scenario.

As the emissions of CO_2, H_2O, and SO_x are directly proportional to the amount of the fuel burned [*Penner et al*., 1999], the changes in the quantity of these emissions under the TRS mirror that of the mission fuel burn. The total global aviation emissions of CO, HC, and NO_x on the other hand all decrease, HC by 0.2 Tg/yr (79%), CO by 0.2 Tg/yr (21%), and NO_x by 0.4 Tg/yr (11%) on average between 2005 and 2011 compared with the original fleet.

Thus, the turboprop replacement strategy investigated is not an efficient scenario in terms of the number of departures needed to carry the original number of passengers. It was shown that despite a doubling in the number of departures, mission fuel burn, and emissions of two important greenhouse gases, CO_2 and H_2O, and the precursor of aerosol formation, SO_x, remained unchanged on average between 2005 and 2011. More importantly, a significant saving in terms of NO_x, CO, and HC emissions was achieved. Turboprops which were at most half the capacity of an average turbofan assuming a 75.5% load factor were used [*Wasiuk et al.,* 2015], but turboprops with a much higher passenger capacity would reduce the number of departures needed. Most flights rarely fly at 100% capacity and thus substituting a turboprop with a slightly smaller capacity can increase load factor which would be an improvement in terms of efficiency and potentially lead to even greater environmental and atmospheric benefits.

3.2. Global Geographical Distribution Changes of Aviation NO_x Emissions Under the TRS

The average (2005–2011) spatial distribution change of the total global aircraft NO_x emissions after swapping turbofan aircraft with turboprop aircraft for short-haul missions (Figure 2) highlights the affected areas of flight activity and major global flight paths between 5.6 and 16.2 km altitude. The allocation of the total global aircraft NO_x emissions between the northern hemisphere (NH) and southern hemisphere (SH) under the TRS is virtually unchanged, with ~90% of the total global aircraft NO_x emissions released in the NH. The distribution of the total global NO_x emissions across the latitudes in the NH changes negligibly as well. The replacement of turbofans with turboprops in regional fleets on a global scale leads to changes in the global geographical distribution of the total global aviation NO_x emissions between 5.6 and 7.2 km (see Figure 2a) when compared with the global geographical distribution of the total global aviation NO_x emissions from the unmodified fleet. The changes between 5.6 and 7.2 km appear to be more or less randomly distributed. Between 7.2 and 9.2 km, the replacement leads to a significant increase in the level of aviation NO_x emissions by up to 500%. These are concentrated in specific regions of the world as seen in Figure 2b. Above 9.2 km, the replacement leads to a decrease in the level of NO_x emissions only with a maximum of 100%. A regional pattern in these changes is discernible which are shown in Figures 2c and 2d.

3.3. Global Vertical Profiles of Fuel Burn, Mission Time, the Distance Flown, and the Emissions of CO, HC, and NO_x

The estimated global mean cruise altitude of the original fleet between 2005 and 2011 was ~10 km. The hypothetical replacement of turbofans with turboprops in regional fleets on a global scale leads to a lowering

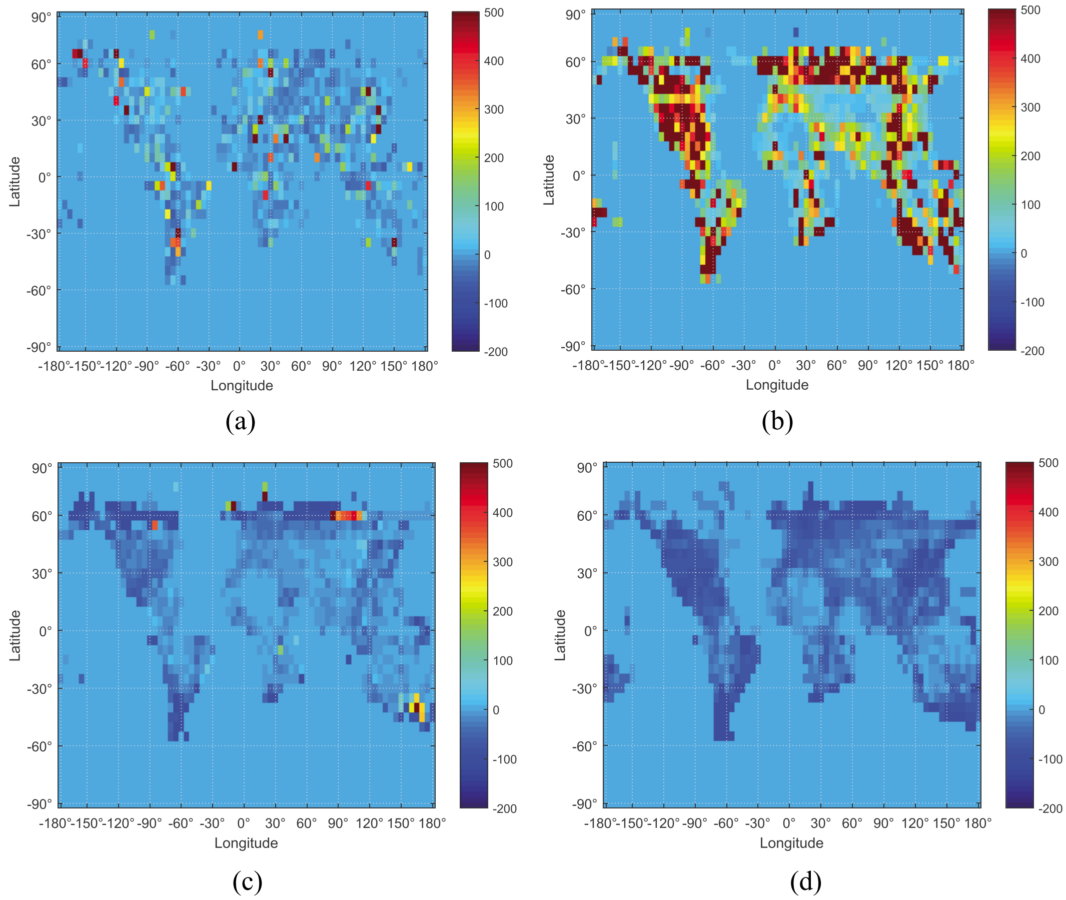

Figure 2. The global geographical distribution of the average (2005–2011) percent change in the total global aviation NO_x emissions under the TRS (a) 5.6–7.2 km, (b) 7.2–9.2 km, (c) 9.2–11.8 km, and (d) 11.8–16.2 km.

of the global mean cruise altitude of approximately 2.7 km which has a significant effect on the global vertical distribution changes of the fuel burned, mission time, the distance flown, and the aircraft emissions of CO, HC, and NO_x for the time period of 2005–2011 (Figure 3). In this study, we used low resolution of the vertical distributions of the global aircraft NO_x emissions and found the shape of the vertical profiles of NO_x emissions between 2005 and 2011 under the TRS with a substantial reduction of 50% at 11.8–16.2 km, a reduction of 20% at 9.2–11.8 km, and a significant increase of 110% at 7.2–9.2 km on average between 2005 and 2011 (Figure 3f). As the vertical distribution changes of the global total CO_2, H_2O, and SO_x emissions qualitatively mirror that of fuel burn, they are not presented here. *Federal Aviation Administration* [2005] reported that roughly 90% of aircraft emissions except HC (70%) and CO (70%) were produced at cruise, climb, and descent altitude, and the remainder was emitted during landing, takeoff, and ground-level operations. Thus, the most significant positive changes in the vertical distribution of the total global mission fuel burn (up to 200%), mission time (up to 1700%), the distance flown (up to 1100%) and the emissions of CO (up to 270%), and NO_x (up to 110%) are found between 7.2 and 9.2 km (Figure 3) due to the lower estimated global mean cruise altitude resulting from the TRS between 2005 and 2011. The lowering of the global mean turboprop cruise altitude also leads to a decrease in global mission fuel burn, mission time, the distance flown, and the aircraft emissions of CO, NO_x, and HC above 9.2 km. The mission distance and the mission time increase at all altitudes up to 9.2 km because of the increased departures for the time period of 2005 to 2011 (Figures 3b and 3c). The fuel burn under the TRS might be expected to increase at all altitudes up to 9.2 km with increasing mission distance and mission times, but turboprop-equipped aircraft require significantly less runway for takeoff and landing than turbofan powered aircraft of the same size [*SKYbrary*, 2016] resulting in decreases of fuel burn at the lowest model layer. Emissions of CO_2, CO, H_2O, HC, SO_x, and NO_x decrease at the majority of the altitudes (see Figure 3) because of their decreased emissions from efficient turboprop aircraft engine

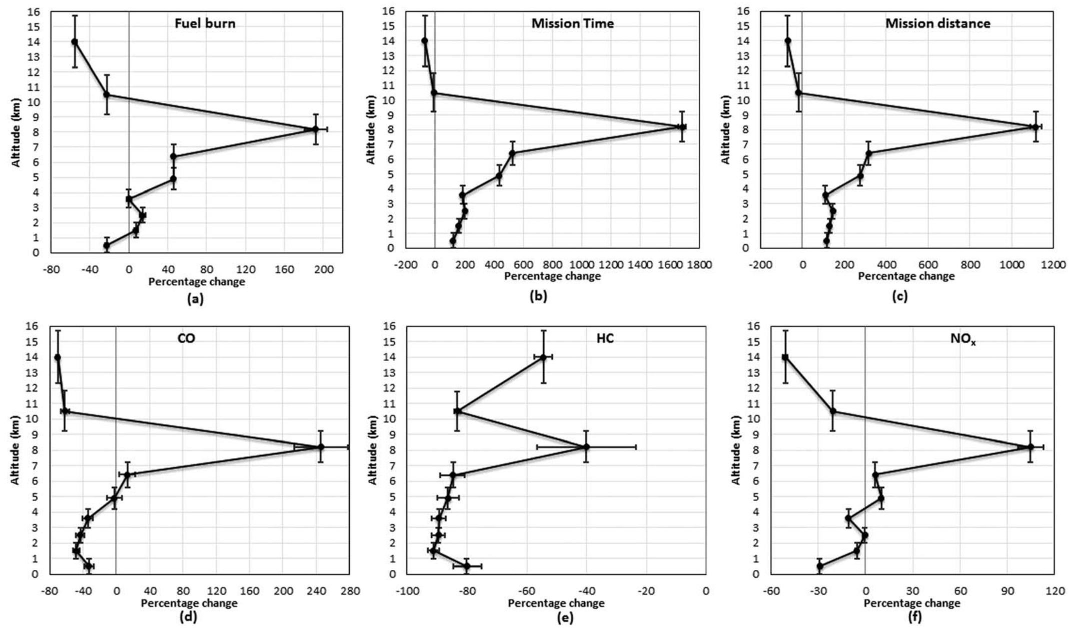

Figure 3. Percent changes in the vertical distribution of the estimated total global (a) mission fuel burn, (b) mission time, (c) distance flown, (d) CO emissions, (e) HC emissions, and (f) NO_x emissions, resulting under the TRS relative to the original fleet during 2005 to 2011. *x* axis error bar represents the standard deviation of the annual total percentage changes across the 7 years. The vertical scale corresponds to the vertical levels in the STOCHEM-CRI model and the vertical point locations represent the midpoint of each model layer, while the *y* axis error bar represents the model layer thickness.

technology within the combustor compared with that of turbofan engines [*George et al.*, 1969]. At ground level, emissions of CO and NO_x decrease by 33 and 29%, respectively, on average between 2005 and 2011. Overall, the contribution of turboprops to atmospheric pollution (e.g., CO_2, H_2O, NO_x, SO_x) is significantly higher at 7.2–9.2 km, but their emissions under the TRS at ground level and upper troposphere (9.2–16.2 km) decrease their atmospheric composition significantly.

3.4. Global Budget of Tropospheric O_3

The substitution of turbofans by turboprops in regional fleets on a global scale decreases the global annual mean burden of NO_x by 4.0 Gg (0.8%) which resulted in a decrease of global annual tropospheric burden of PAN by 1.7 Gg (0.3%). The global annual mean tropospheric burden of O_3 decreased by 0.9 Tg (0.3%) on average between 2005 and 2011, and as a consequence of decreased O_3 levels, the global annual mean tropospheric burden of OH decreases by 0.002 Gg (0.8%). Table 3 shows the global O_3 budget under the TRS in which both total production and loss decrease slightly by 11.6 Tg/yr (0.1%) and 11.1 Tg/yr (0.1%), respectively. Two dominant chemical production channels, $HO_2 + NO$ and $CH_3O_2 + NO$,

Table 3. The Average Absolute and Percent Change in the Global Tropospheric O_3 Budget Terms Simulated by the STOCHEM-CRI Under the TRS During 2005 to 2011

Species	Average Δ (Tg/yr)	Average %Δ
Chemical Production		
$HO_2 + NO$	−9.6	−0.2
$CH_3O_2 + NO$	−1.7	−0.1
$CH_3CO_3 + NO$	−0.1	−0.0
Isoprene peroxy + NO	0.0	0.0
$HOCH_2CH_2O_2 + NO$	−0.0	−0.0
Other $RO_2 + NO$	−0.1	−0.0
Other	−0.1	−0.1
Stratospheric influx	0.0	0.0
Total production	−11.6	−0.1
Chemical Loss		
$O(^1D) + H_2O \rightarrow 2OH$	−3.1	−0.1
$HO_2 + O_3 \rightarrow OH + 2O_2$	−1.0	−0.1
$OH + O_3 \rightarrow HO_2 + O_2$	−3.5	−0.5
Other	−0.5	−0.1
Dry deposition	−3.0	−0.1
Total loss	−11.1	−0.1
Production − loss	−0.5	−0.6

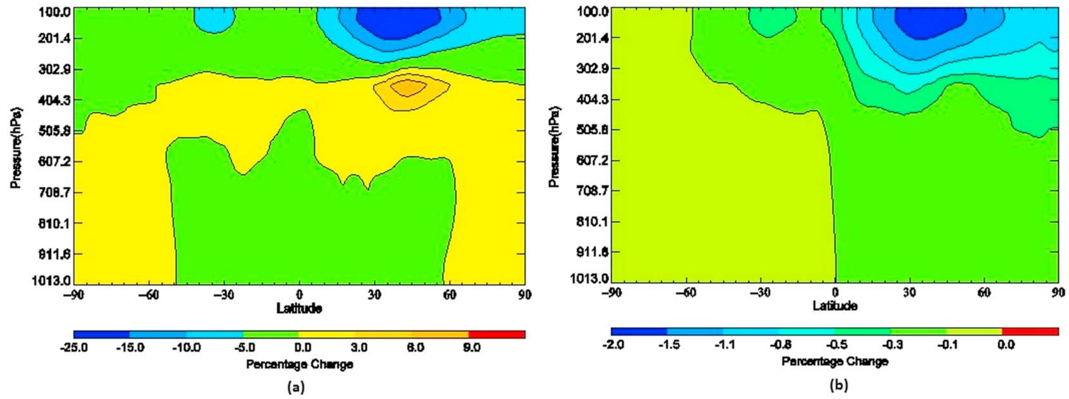

Figure 4. Global zonal distribution of the average percent changes in (a) NO_x and (b) O_3 under the TRS for the seven sensitivity simulations (2005–2011).

decrease by 9.6 Tg/yr (0.2%) and 1.7 Tg/yr (0.1%) respectively, while the other channels remain unchanged. There is a decrease in all channels that make up the chemical loss, the most being OH + O_3 at 3.5 Tg/yr (0.5%). Net O_3 production decreases by 0.5 Tg/yr (0.6%) on average under the TRS. In the NO_x-saturated regime (taxi out, takeoff, approach, landing, and taxi-in phases when VOC/NO_x ratio is small), the decreased NO_x at ground level under TRS (Figure 3f) leads to no significant change in O_3 mixing ratios. However, in the NO_x sensitive regime (ascent, cruise, and descent phases when VOC/NO_x ratio is high), the significant decrease in NO_x at 9.2–16.2 km (Figure 3f) reduces O_3 mixing ratios notably. There is an overall reduction in levels of tropospheric O_3 after substitution of turbofans by turboprops on a global scale in regional fleets on short-haul missions which would be an improvement in terms of environmental pollution.

3.5. Global Geographical NO_x and O_3 Distribution

Figure 4 shows the global zonal distribution of the average percent changes in NO_x and O_3 mixing ratios under the TRS. Following the replacement of turbofans by turboprops in regional fleets on a global scale and consequently lowering the estimated global mean cruise altitude, the concentration of NO_x is generally suppressed by 5–10% above 9.2 km in the NH. In particular, there are two areas of greatest negative changes: one of up to 10% between 30°S and 40°S in the SH and one of up to 25% between 25°N and 55°N in the NH at 11.8–16.2 km as seen in Figure 4. Brazil and southern coast of Australia emerge as new NO_x mixing ratio hot spots during 2005–2011 [*Wasiuk et al.*, 2016a]; the TRS replacement strategy reduces the NO_x change in Brazil and Australia mostly which reflects the negative NO_x change in the SH. Between 7.2 and 9.2 km NO_x mixing ratios are increased by up to 8% which can be attributed to the lowering of the global mean cruise altitude under the TRS.

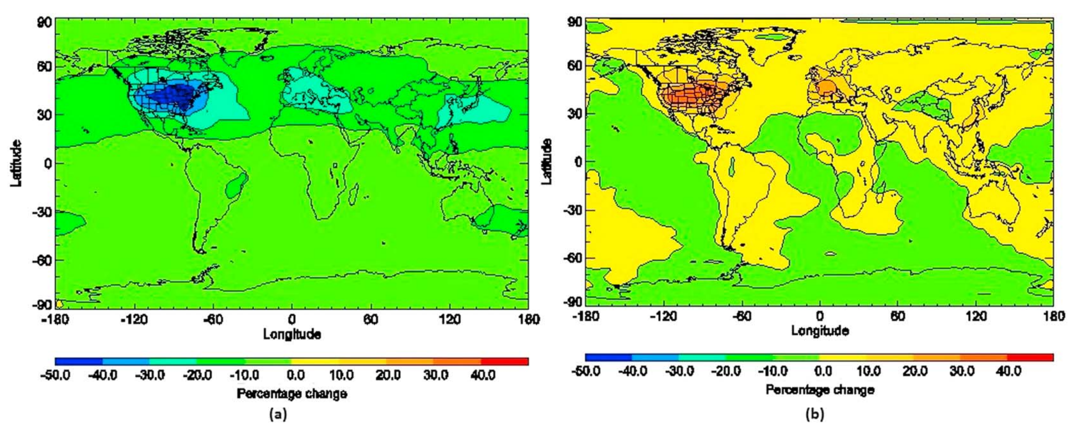

Figure 5. Global geographical distribution of the average percentage change in NO_x mixing ratios under the TRS for the seven sensitivity simulations (2005–2011) (a) between 11.8 and 16.2 km and (b) between 7.2 and 9.2 km.

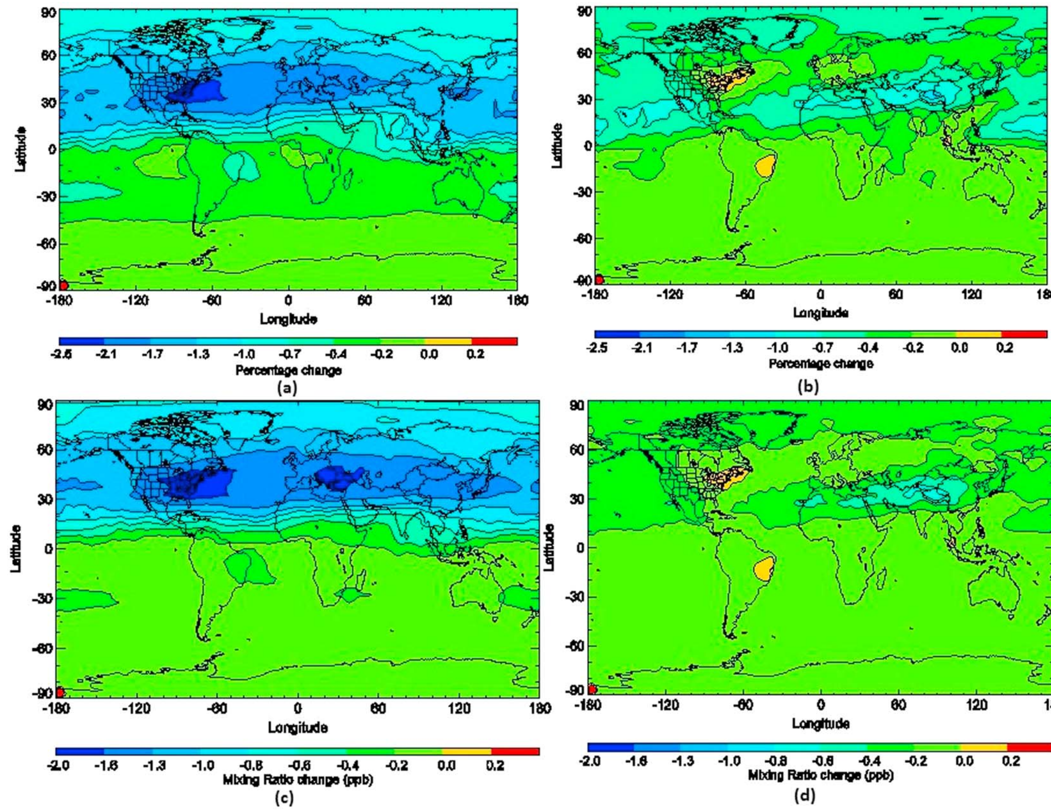

Figure 6. Global geographical distribution of the average percentage changes in O_3 mixing ratios under the TRS for 2005–2011 (a) between 11.8 and 16.2 km and (b) between 7.2 and 9.2 km. Global geographical distribution of the absolute changes in O_3 mixing ratios under the TRS for 2005–2011 (c) between 11.8 and 16.2 km and (d) between 7.2 and 9.2 km.

Following the reduction in NO_x concentrations due to the substitution of turbofans by turboprops in regional fleets on a global scale, overall O_3 mixing ratios decrease and most notably between 10°N and 90°N starting at 9.2 km (Figure 4b). The greatest decrease (≥2%) takes place at 11.8–16.2 km, between 25°N and 50°N. When averaged zonally, no increase in O_3 mixing ratios corresponding to the increases in NO_x concentrations is seen between 7.2 and 9.2 km.

The global geographical distribution and magnitude of the NO_x changes under the TRS at 11.8–16.2 km and 7.2–9.2 km are shown in Figure 5. Globally, the reduction in NO_x mixing ratios at 11.8–16.2 km is found to be 8% and regionally up to 50% reduction has been found over the North American east coast (Figure 5a). Figure 5b shows the positive changes in the geographical distribution of NO_x at 7.2–9.2 km where the global mean change (2%) and the regional change (up to 40% in central mainland Europe, and t*he* east coast of North America) have been observed.

The decreased aircraft NO_x emissions at 11.8–16.2 km (NO_x sensitive region) under the TRS leads to a decrease in global mean O_3 mixing ratios by 0.8% and regional O_3 mixing ratios by up to 2.5% (2 ppb) over the North American east coast (Figures 6a and 6c), but the aircraft emit an increased amount of NO_x at 7.2–9.2 km (NO_x sensitive region) under TRS where the additional NO_x leads to a decrease in global mean O_3 mixing ratios by 0.3% and an increase in regional O_3 mixing ratios by up to 0.2% (2 ppb) North Atlantic Ocean, southern Europe, and south East Asia (Figures 6b and 6d). The increases in the concentration of O_3 are found between 7.2 and 9.2 km due to the lowering of the estimated global mean cruise altitude and the displacement of the total global aviation NO_x emissions to a lower altitude materialize away from the continents and over the oceans. A belt of decreased O_3 levels at 0–30°N stretches from the east to the west (Figure 6b); hence, despite increased NO_x levels between 7.2 and 9.2 km, there are negative changes in O_3 levels (1%) in this region. In terms of the impact on the global climate, the turboprop replacement strategy resulted in an average overall decrease of O_3 in the entire modeling domain, in particular, nearest to the tropopause where the radiative forcing of O_3 is strongest [*Brasseur et al.*, 1998]. This is likely to be in a regime closer to the net O_3 production compensation point (the point at which the net O_3 production is equal to zero), which is preferable in terms of the atmospheric impact. The findings in the study are in qualitative agreement with the results of *Grewe et al.* [2002] and *Søvde et al.* [2014] where they found reduced levels of O_3 after lowering the cruise altitude by 1 km and 0.6 km, respectively. However the magnitudes of O_3 changes cannot be compared because of the different methodology used and the smaller altitude decrease considered in the *Grewe et al.* [2002] and *Søvde et al.* [2014] studies. We have not assessed the potential of TRS strategy on the long-term effects of NO_x emissions, effects of CO_2 emissions, changes in contrail coverage, or aircraft-produced aerosol emissions. However, considering the relationship of the radiative forcing with the cruise altitude [*Søvde et al.*, 2014], it can be concluded that the TRS strategy reduces the global O_3 levels by up to 2 ppb (Figure 6c) which subsequently reduces the radiative forcing (RF) by 2–3 mW m^{-2}. The total RF from aviation (in 2005, excluding cirrus effects) is ~55 mW m^{-2} [*Lee et al.*, 2009], i.e., the mitigation strategy may reduce total aviation RF by ~5%.

4. Conclusion

A theoretical mitigation strategy for commercial aircraft impact on tropospheric composition referred to as the turboprop replacement strategy (TRS), where all turbofans on short-haul routes were replaced with existing turboprops, was investigated in the study. With increasing the number of global departures under TRS, the global levels of emissions of CO_2, H_2O, and SO_x changed in line with mission fuel burn, i.e., remained approximately unchanged on average between 2005 and 2011, while total global aviation CO, HC, and NO_x emissions were reduced by 79, 21, and 11% on average between 2005 and 2011. TRS would lead to an estimated lowering of the global mean cruise altitude of flights up to 1700 NM by approximately 2.7 km which resulted in significant changes in the global geographical distribution of the total global aviation emissions above 7.2 km. At ground level, NO_x and CO mixing ratios were reduced by 29 and 33%, respectively, between 2005 and 2011.

The manipulation of the aviation NO_x emissions between 2005 and 2011 due to TRS has the effect of decreasing the tropospheric burden of O_3 by 0.9 Tg. The net O_3 production decreases by 0.5 Tg (0.6%) between 2005 and 2011. TRS leads to a substantial decrease of NO_x mixing ratios at the current estimated mean cruise altitude near the tropopause. The displacement of the total annual global aviation NO_x emissions to the lower altitude between 7.2 and 9.2 km leads to an overall decrease of O_3 at that altitude. The findings from this study imply that the substitution of turbofans with turboprops on a global scale in regional fleets on short haul missions would lead to an overall reduction in levels of tropospheric O_3 in a region of the atmosphere where it is most harmful in terms of the radiative forcing of climate change.

A reduction in surface NO_x, CO, and HC local to airports is a matter of much current debate, but it should be noted that studies have shown that there is a direct relationship between such compounds and negative health outcomes and that such exposure can have long-term impacts [*Janke et al.*, 2009; *Hansell et al.*, 2015], and so any reduction in primary emissions would be welcome. The global model used here will not be able to resolve changes in O_3 on city wide and regional scales and so O_3 may increase during outflow as the airport is likely to be in a NO_x-saturated, VOC-limited environment, but total O_3 production will scale approximately with NO_x away from urban areas and so any reduction in NO_x is likely to reduce surface O_3 regionally with multiple health benefits for animals, plants, and building structures [e.g., *Jenkin and Clemitshaw*, 2000].

Acknowledgments
We thank Michael Cooke (Met Office, UK), Alan Knights (University of Bristol, UK), and Steven Utembe (University of Melbourne, Australia) for their supports with STOCHEM integrations. We also thank the Engineering and Physical Sciences Research Council (EPSRC) (grant EP/5011214), the Natural Environment Research Council (NERC) (grant NE/J009008/1 and NE/I014381/1), and Faculty of Engineering and School of Chemistry, University of Bristol for funding various aspects of this work. The airline schedule data used in the analysis are available for purchase from CAPSTATS (http://www.capstats.com). Aircraft performance model data, i.e., airframe and operation specific data including aircraft codes, are from EUROCONTROL BADA (Base of Aircraft DAta): http://www.eurocontrol.int/services/bada; these are IATA codes and are translated to ICAO aircraft codes using http://www.airlinecodes.co.uk/arctypes.asp. Engine names are primarily taken from the EUROCONTROL BADA model; where missing are they taken from SKYbrary: http://www.skybrary.aero/index.php/Main_Page as are aircraft capacity and range data. Engine data are taken from the ICAO Aircraft Engine Databank: https://www.easa.europa.eu/document-library/icao-aircraft-engine-emissions-databank The Boeing Fuel Flow Model 2 (BFFM2) algorithm is from SAE Aerospace using http://standards.sae.org. Additional data for the Aircraft Fuel Burn and Emissions Inventory are available from the authors upon request (m.lowenberg@bristol.ac.uk).

References

Air Transport Action Group (2010), Beginner's guide to aviation efficiency, Air Transport Action Group, Switzerland. [Available at www.atag.org/component/downloads/downloads/59.htm, (last accessed 11/02/2016).]

Babikian, R., S. P. Lukachko, and I. A. Waitz (2002), The historical fuel efficiency characteristics of regional aircraft from technological, operational, and cost perspectives, *J. Air Transp. Manage.*, *8*, 389–400.

Brasseur, G. P., R. A. Cox, D. Hauglustaine, I. Isaksen, J. Lelieveld, D. H. Lister, R. Sausen, U. Schumann, A. Wahner, and P. Wiesen (1998), European scientific assessment of the atmospheric effects of aircraft emissions, *Atmos. Environ.*, *32*, 2329–2418.

Burkhardt, U., and B. Kärcher (2011), Global radiation forcing from contrail cirrus, *Nat. Clim. Change*, *1*, 54–58.

Collins, W. J., S. Stevenson, C. E. Johnson, and R. G. Derwent (1997), Tropospheric ozone in a global scale three dimensional Lagrangian model and its response to NO_x emission controls, *J. Atmos. Chem.*, *26*, 223–274.

Derwent, R. G., D. S. Stevenson, R. M. Doherty, W. J. Collins, M. G. Sanderson, and C. E. Johnson (2008), Radiative forcing from surface NO_x emissions: spatial and seasonal variations, *Clim. Change*, *88*, 385–401.

Erzberger, H., J. D. McLean, and J. F. Barman (1975), Fixed-range optimum trajectories for short-haul aircraft, *NASA Tech. Note D-8115*, pp. 1–10, Natl. Aeron. and Space Admin., Washington, D. C.

EUROCONTROL (2016), Aircraft Performance Database. [Available at https://contentzone.eurocontrol.int/aircraftperformance/default.aspx?, (last accessed 11/02/2016).]

Federal Aviation Administration (2005), Aviation and emissions. A Primer, January 2005. Federal Aviation Administration Office of Environment and Energy. [Available at http://www.faa.gov/regulations_policies/policy_guidance/envir_policy/media/aeprimer.pdf (last accessed 11/02/2016).]

George, R. E., J. A. Verssen, and R. L. Chass (1969), Jet aircraft: A growing pollution source, *J. Air Pollut. Cont. Assoc.*, *19*, 847–855.

Gilmore, C. K., S. R. H. Barrett, J. Koo, and Q. Wang (2013), Temporal and spatial variability in the aviation NO_x-related O_3 impact, *Environ. Res. Lett.*, *8*, 034027, 8.

Granier, C., J. F. Lamarque, A. Mieville, J. F. Muller, J. Olivier, J. Orlando, J. Peters, G. Petron, S. Tyndall, and S. Wallens (2005), POET, a database of surface emissions of ozone precursors. [Available at http://accent.aero.jussieu.fr/POET_metadata.php, (last accessed 11/02/2016).]

Grewe, V., M. Dameris, C. Fichter, and D. S. Lee (2002), Impact of aircraft NO_x emissions. Part 2: Effects of lowering the flight altitude, *Meterol. Z.*, *11*, 197–205.

Hansell, A., R. E. Ghosh, M. Blangiardo, C. Perkins, D. Vienneau, K. Goffe, D. Briggs, and J. Gulliver (2015), Historic air pollution exposure and long-term mortality risks in England and Wales: Prospective longitudinal cohort study, *Thorax*, 1–9.

Houweling, S., F. Dentener, J. Lelieveld, B. Walter, and E. Dlugokencky (2000), The modeling of tropospheric methane—How well can point measurements be reproduced by a global model?, *J. Geophys. Res.*, *105*, 8981–9002, doi:10.1029/1999JD901149.

Janke, K. M., C. Propper, and J. Henderson (2009), Do current levels of air pollution kill? The impact of air pollution on population mortality in England, *Health Econ.*, *18*, 1031–1055.

Jenkin, M. E., and K. C. Clemitshaw (2000), Ozone and other secondary photochemical pollutants: Chemical processes governing their formation in the planetary boundary layer, *Atmos. Environ.*, *34*, 2499–2527.

Jenkin, M. E., L. A. Watson, S. R. Utembe, and D. E. Shallcross (2008), A Common Representative Intermediates (CRI) mechanism for VOC degradation. Part 1: Gas phase mechanism development, *Atmos. Environ.*, *42*, 7185–7195.

Khan, M. A. H., et al. (2014), Reassessing the photochemical production of methanol from peroxy radical self and cross reactions using the STOCHEM-CRI global chemistry and transport model, *Atmos. Environ.*, *99*, 77–84.

Köhler, M. O., G. Rädel, K. P. Shine, H. L. Rogers, and J. A. Pyle (2013), Latitudinal variation of the effect of aviation NO_x emissions on atmospheric ozone and methane and related climate metrics, *Atmos. Environ.*, *64*, 1–9.

Lee, D. S., D. W. Fahey, P. M. Forster, P. J. Newton, R. C. N. Wit, L. L. Lim, B. Owen, and R. Sausen (2009), Aviation and global climate change in the 21st century, *Atmos. Environ.*, *43*, 3520–3537.

Mikaloff-Fletcher, S. E., P. P. Tans, L. M. Bruhwiler, J. B. Miller, and M. Heimann (2004), CH_4 sources estimated from atmospheric observations of CH_4 and its $^{13}C/^{12}C$ isotopic ratios: 1. Inverse modeling of source processes, *Global Biogeochem. Cycles*, *18*, GB4004, doi:10.1029/2004GB002223.

Mrazova, M. (2013), *Innovations, Technology and Efficiency Shaping the Aerospace Environment*, vol. 5, pp. 91–99, INCAS Bull., Romania

Nygren, E. (2008), Aviation fuels and peak oil, Master's thesis, Uppsala Univ., Sweden.

Olsen, S. C., et al. (2013), Comparison of model estimates of the effects of aviation emissions on atmospheric ozone and methane, *Geophys. Res. Lett.*, *40*, 6004–6009, doi:10.1002/2013GL057660.

Peace, H., J. Maughen, B. Owen, and D. Raper (2006), Identifying the contribution of different airport related sources to local urban air quality, *Environ. Modell. Software*, *21*, 532–538.

Penner, J. E., D. H. Lister, D. J. Griggs, D. J. Dokken, and M. McFarland (Eds) (1999), Aviation and the global atmosphere, in *A Special Report of Working Groups I and III of the Intergovernmental Panel on Climate Change (IPCC)*, pp. 373, Cambridge Univ. Press, Cambridge, U. K.

Pitari, G., E. Mancini, and A. Bregman (2002), Climate forcing of subsonic aviation: Indirect role of sulfate particles via heterogeneous chemistry, *Geophys. Res. Lett.*, *29*(22), 2057, doi:10.1029/2002GL015705.

Rogers, H. L., D. S. Lee, D. W. Raper, P. M. deF Foster, C. W. Wilson, and P. J. Newton (2002), The impacts of aviation on the atmosphere, *Aeronaut. J.*, *106*, 521–546.

Ryerson, M. S., and M. Hansen (2010), The potential of turboprops for reducing aviation fuel consumption, *Transp. Res. Part D: Transp. Environ.*, *15*, 305–314.

Schumann, U. (2002), Contrail Cirrus, in *Cirrus*, edited by D. Lynch et al., pp. 231–255, Oxford Univ. Press, Oxford.

Skowron, A., D. S. Lee, and R. R. De León (2015), Variation of radiative forcings and global warming potentials from regional aviation NO_x emissions, *Atmos. Environ.*, *104*, 69–78.

SKYbrary (2016), [Available at http://www.skybrary.aero/index.php/, (last accessed 11/02/2016).]

Søvde, O. A., et al. (2014), Aircraft emission mitigation by changing route altitude: A multi-model estimate of aircraft NO_x emission impact on O_3 photochemistry, *Atmos. Environ.*, *95*, 468–479.

Stevenson, D. S., and R. G. Derwent (2009), Does the location of aircraft nitrogen oxide emissions affect their climate impact?, *Geophys. Res. Lett.*, *36*, L17810, doi:10.1029/2009GL039422.

Stevenson, D. S., R. M. Doherty, M. G. Sanderson, W. J. Collins, C. E. Johnson, and R. G. Derwent (2004), Radiative forcing from aircraft NO_x emissions: Mechanisms and seasonal dependence, *J. Geophys. Res.*, *109*, D17307, doi:10.1029/2004JD004759.

Utembe, S. R., L. A. Watson, D. E. Shallcross, and M. E. Jenkin (2009), A common representative intermediates (CRI) mechanism for VOC degradation. Part 3: Development of a secondary organic aerosol module, *Atmos. Environ.*, *43*, 1982–1990.

Utembe, S. R., M. C. Cooke, A. T. Archibald, M. E. Jenkin, R. G. Derwent, and D. E. Shallcross (2010), Using a reduced Common Representative Intermediates (CRIv2-R5) mechanism to simulate tropospheric ozone in a 3-D Lagrangian chemistry transport model, *Atmos. Environ.*, *44*, 1609–1622.

Wasiuk, D. K. (2014), Modelling aircraft emissions and their impact on atmospheric composition and ozone, PhD thesis, Univ. of Bristol, Bristol, U. K.

Wasiuk, D. K., M. H. Lowenberg, and D. E. Shallcross (2015), An aircraft performance model implementation for the estimation of global and regional aviation fuel burn and emissions, *Transp. Res. Part D: Transp. Environ.*, *35*, 142–159.

Wasiuk, D. K., M. A. H. Khan, D. E. Shallcross, and M. H. Lowenberg (2016a), The impact on tropospheric composition changes of global aviation NO_x emissions from 2005 to 2011, *Atmos. Res.*, *178-179*, 73–83.

Wasiuk, D. K., M. A. H. Khan, D. E. Shallcross, and M. H. Lowenberg (2016b), A commercial aircraft fuel burn and emissions inventory for 2005–2011, *Atmosphere*, *7*, 78.

Watson, L. A., D. E. Shallcross, S. R. Utembe, and M. E. Jenkin (2008), A Common Representative Intermediates (CRI) mechanism for VOC degradation. Part 2: Gas phase mechanism reduction, *Atmos. Environ.*, *42*, 7196–7204.

Yu, K. N., Y. P. Cheung, T. Cheung, and R. C. Henry (2004), Identifying the impact of large urban airports on local air quality by nonparametric regression, *Atmos. Environ.*, *38*, 4501–4507.